

## Optical Frequency Synthesizer for Precision Spectroscopy

R. Holzwarth, Th. Udem, and T. W. Hänsch

*Max-Planck-Institut für Quantenoptik, Hans-Kopfermann-Straße 1, 85748 Garching, Germany*

J. C. Knight, W. J. Wadsworth, and P. St. J. Russell

*Optoelectronics Group, Department of Physics, University of Bath, Claverton Down, Bath BA2 7AY, United Kingdom*

(Received 4 May 2000)

We have used the frequency comb generated by a femtosecond mode-locked laser and broadened to more than an optical octave in a photonic crystal fiber to realize a frequency chain that links a 10 MHz radio frequency reference phase-coherently in one step to the optical region. By comparison with a similar frequency chain we set an upper limit for the uncertainty of this new approach to  $5.1 \times 10^{-16}$ . This opens the door for measurement and synthesis of virtually any optical frequency and is ready to revolutionize frequency metrology.

PACS numbers: 32.30.Jc, 06.30.Ft, 42.62.Eh

For precision optical spectroscopy one has to determine optical frequencies of several 100 THz in terms of the definition of the SI second represented by the cesium ground state hyperfine splitting at 9.2 GHz. In the past heroic efforts were required to measure optical frequencies with harmonic frequency chains which create successive harmonics from the cesium radio frequency reference. These frequency chains were large, delicate to handle and usually designed to measure only one particular optical frequency [1–4]. Because of the  $10^5$  times higher frequencies and the narrow width of selected optical transitions, it is worthwhile to consider atomic clocks based on such optical transitions. The major obstacle for the construction of optical clocks has been the fact that no reliable clockwork was available that could count these rapid oscillations. Projected accuracies for optical frequency standards reach the  $10^{-18}$  level and put up extraordinary demands on this clockwork. The  $f:2f$  interval frequency chain [5–7] using a femtosecond (fs) frequency comb finally provides the missing clockwork in a compact and reliable setup.

It has been long recognized that the periodic pulse train of a mode-locked laser can be described in the frequency domain as a comb of equidistant modes. Such a comb can be used to measure large optical frequency differences by counting modes if the spacing between them is known [8]. As the spectral width of these lasers scales inversely with the pulse duration the advent of fs lasers has opened the possibility to directly access THz frequency gaps [9,10]. Previously we have shown that the easily accessible repetition rate of such a laser equals the mode spacing within the experimental uncertainty of a few parts in  $10^{16}$  [11] and that the frequency comb is equally spaced even after further spectral broadening in a standard single mode fiber on the level of a few parts in  $10^{18}$  [12]. Extending this principle of determining frequency differences to the intervals between harmonics of optical frequencies [13] leads naturally to the absolute measurement of optical frequencies. The first frequency chain following this principle has been used in a recent determination of the hydrogen  $1S-2S$  transition and

measured the interval between  $3.5f$  and  $4f$  where  $f$  is the frequency of a HeNe laser at  $3.39 \mu\text{m}$  (88.4 THz) [5].

The latest developments in photonic crystal fibers (PCF) [14–17], with specifically engineered wave guiding and dispersion properties, allow very efficient spectral broadening of fs pulses to more than one optical octave. It has been demonstrated that such a broad comb can be used as a freely floating ruler to directly measure the frequency interval between the fundamental ( $f$ ) and the second harmonic ( $2f$ ) of a Nd:YAG laser at 1064 nm/532 nm locked to an iodine transition [6]. To exploit the full potential of this approach we have now used such a broadened frequency comb to stabilize the frequency interval between a laser frequency  $f$  and its second harmonic  $2f$ , and therefore the frequency  $f = 2f - f$  itself. Alternatively, the comb itself can be frequency doubled [6,7,18]. At the end point of this development we have arrived at a frequency chain that consists of one fs laser and an optional Nd:YAG laser only and nevertheless links a 10 MHz rf reference phase coherently in one step to almost  $10^6$  distinct optical frequencies. To evaluate the performance of such a frequency chain we report in this Letter on the comparison of two such chains, setting an upper limit of  $5.1 \times 10^{-16}$  for their uncertainties.

To understand the mode structure of a fs frequency comb, consider a pulse circulating in a laser cavity with length  $L$  at a carrier frequency  $f_c$  that is subject to strong amplitude modulation described by an envelope function  $A(t)$ . This function defines the pulse repetition time  $T = f_r^{-1}$  by demanding  $A(t) = A(t - T)$  where  $T$  is calculated from the cavity mean group velocity:  $T = 2L/v_{gr}$ . Fourier transformation of  $A(t)$  shows that the resulting spectrum consists of a comb of laser modes separated by the pulse repetition frequency and centered at  $f_c$  [19]. Since  $f_c$  is not necessarily an integer multiple of  $f_r$ , the modes are shifted from being exact harmonics of the pulse repetition frequency by an offset  $f_o < f_r$ :

$$f_n = nf_r + f_o, \quad n = \text{a large integer.} \quad (1)$$

This equation maps two radio frequencies  $f_r$  and  $f_o$  onto the optical frequencies  $f_n$ . While  $f_r$  is readily measurable,  $f_o$  is not easily accessible unless the frequency comb contains more than an optical octave [19]. In the time domain the frequency offset is obvious because group velocity differs from phase velocity, and therefore the carrier wave does not repeat itself after one round trip but appears phase shifted by, say,  $\Delta\varphi$ . The offset frequency is then calculated from  $f_o = \Delta\varphi/T2\pi$  [19]. To compensate for small frequency drifts caused, for example, by acoustics or temperature variations of the fiber we control the absolute position and the mode separation with beat signals obtained after the fiber.

Our PCF is a strongly guiding fiber waveguide that uses an array of submicron-sized air holes running the length of a silica fiber to confine light to a pure silica region embedded within the array [14]. The large refractive index contrast between the pure silica core and the “holey” cladding and the resultant strong optical confinement allow the design of fibers with very different characteristics from those of conventional fibers. In the fiber used here, a very small core diameter of approximately  $1.5 \mu\text{m}$  leads to increased nonlinear interaction of the guided light with the silica. At the same time the very strong waveguide dispersion substantially compensates the material dispersion of the silica at wavelengths below  $1 \mu\text{m}$  [15]. This gives an overall group velocity dispersion (GVD) which is zero around 700 nm. The absolute value of the GVD over much of the visible and near-infrared range is smaller than in conventional fibers, and the GVD is anomalous at much shorter wavelengths. As a result, fs pulses travel farther in these fibers before being dispersed, which further increases the nonlinear interaction. Consequently, substantially broader spectra can be generated in PCFs at relatively low peak powers [16,17]. The creation of additional modes by the fiber action can be understood by self-phase modulation or alternatively in the frequency domain by four wave mixing. Although self-phase modulation is likely the dominant mechanism of spectral broadening, there are other processes like stimulated Raman and Brillouin scattering or shock wave formation that might spoil the usefulness of these broadened frequency combs. And, indeed, in an experiment using 8 cm of PCF and 73 fs pulses at 75 MHz repetition rate from a Mira 900 system (Coherent Inc.) we have seen an exceptionally broad spectrum from 450 to 1400 nm, but we have not been able to observe beat notes with a signal to noise ratio sufficient for phase locking. We did not observe these problems with a higher repetition rate and shorter pulse length. So far we have not encountered any degradation of the fiber as one might expect due to the high peak intensities.

The  $f:2f$  interval frequency chain sketched in Fig. 1 is based on a Ti:sapphire ring laser with a bandwidth supporting 25 fs and a 625 MHz repetition rate (GigaOptics, model GigaJet). While the ring design makes it almost immune to feedback from the fiber, the high repetition rate increases the available power per mode. The highly effi-

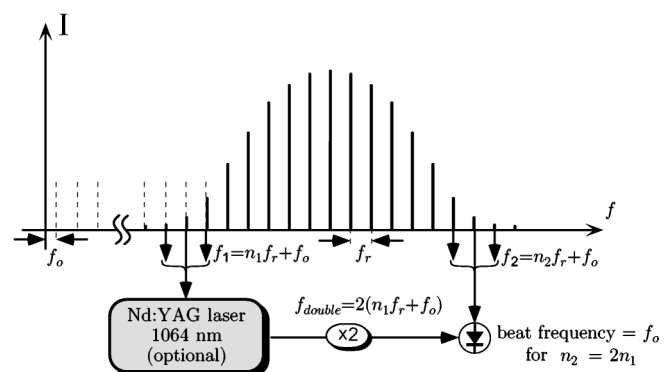


FIG. 1. The  $f:2f$  interval frequency chain is based on the stabilization of the interval between an optical frequency  $f$  and its second harmonic  $2f$  with the help of a fs frequency comb. Once the offset frequency and repetition rate are locked, all the modes in the comb can be used for optical frequency measurements.

cient spectral broadening of the PCF compensates for the decrease of available peak power connected with a high repetition rate. To generate an octave spanning comb we have coupled 190 mW average power through 35 cm PCF. In our experiments we have used two repetition rates, 625 and 624.87 MHz, two offset frequencies  $f_o = 0$  Hz and 64 MHz, as well as operation with and without an auxiliary frequency doubled Nd:YAG laser (InnoLight, model Prometheus) defining the frequencies  $f$  and  $2f$ .

We lock the pulse repetition frequency  $f_r$  to the rf reference provided by a 10 MHz quartz oscillator (Oscilloquartz, model 8607-BM) by controlling the fs laser cavity length with a piezomounted folding mirror. To reduce noise in the detection process we use a 12.5 GHz signal provided by a synthesizer (Hewlett-Packard, model 8360) to phase lock the 20th harmonic of  $f_r$  [9,19]. Then the fundamental wave  $f_{1064}$  of the Nd:YAG laser is locked to one of the modes of the frequency comb by forcing their beat note to oscillate in phase with a radio frequency reference  $LO_{1064}$ , the local oscillator [19,20]. As shown in Fig. 1 we then observe a beat note at  $2f_{1064} = f_{532} = 2(nf_r + f_o - LO_{1064})$  with the frequency comb whose closest mode frequency is given by  $2nf_r + f_o$ . The beat frequency  $f_o - 2LO_{1064}$  is locked to another local oscillator:  $f_o - 2LO_{1064} = -LO_{532}$ . This is accomplished by adjusting the power of the pump laser (Coherent, model Verdi) with an electro-optic modulator (Gsänger, LM0202) [12,21]. Primarily this changes the mean power of the fs laser and thus the optical path length in the Ti:sapphire crystal via its optical Kerr effect. Although the two controls (i.e., cavity length and pump power) are not orthogonal, they affect the round trip group delay  $T$  and the round trip phase delay differently, and this is what is needed [19]. Note that for the case  $f_o = 0$  Hz according to Eq. (1) the mode frequencies are exact harmonics of the repetition rate. By choosing the value of  $2LO_{1064} - LO_{532} = f_o = \Delta\varphi/T2\pi$  we can adjust the pulse to pulse phase shift  $\Delta\varphi$  to a selected value (e.g.,  $\Delta\varphi = 0$ ). We have therefore precise control of the

time evolution of the absolute carrier phase versus the envelope. Stabilization of  $f_o$  is in turn a prerequisite for the next generation of ultrafast experiments making use of few cycle driven high field processes [7,18]. However, the ultimate carrier-to-envelope phase control, i.e., the control over  $\varphi$  rather than  $\Delta\varphi$ , has not yet been achieved.

For the second operating mode we directly frequency double the infrared part of the spectrum around 1060 nm and observe a beat note with the green part [6,7]. The infrared part of the spectrum is separated from the green part with the help of a dichroic mirror, doubled in a  $3 \times 3 \times 7$  mm<sup>3</sup> KTP (potassium titanyl phosphate) crystal properly cut and antireflection coated and recombined with the green part on a polarizing beam splitter. For the green part an optical delay line is included to match the optical path lengths. The polarization axes of the recombined light are mixed using a rotatable polarizer. A grating which serves as 5 nm wide bandpass filter selects the wavelengths around 530 nm. A beat signal with a signal to noise ratio exceeding 40 dB in 400 kHz bandwidth, sufficient for phase locking [12], has been obtained. In this way we have direct access to the offset frequency  $f_o$  that we have locked to 64 MHz using the offset locking technique described above, although any other value is possible.

To check the integrity of the broad frequency comb and evaluate the overall performance of the  $f:2f$  interval frequency chain we compare it with a similar frequency chain that has already been used in a recent comparison of the hydrogen  $1S-2S$  transition frequency (at 121 nm) with a cesium fountain clock [22]. This chain was modified to replace a dye laser by a frequency doubled diode laser/tapered amplifier combination at 969 nm [23] and by removing an additional frequency gap of 1 THz by operating the diode laser at exactly  $3.5f$  where  $f$  is the frequency of a HeNe laser at 88.4 THz (3.39  $\mu$ m). The 44.2 THz frequency comb used here is generated by a Mira 900 system with a regular single mode fiber and has been thoroughly tested [11,12]. It is used to stabilize the frequency gap set by two diode lasers at  $3.5f$  and  $4f$  as sketched in Fig. 2. This relates the difference  $4f - 3.5f = 0.5f$  and therefore  $f$  to the rf source controlling the repetition rate. A frequency interval divider [24] fixes the relation between the frequencies  $f$ ,  $4f$ , and  $7f$ , and additional nonlinear steps are used to generate  $4f$  and  $3.5f$ . Just like the simple  $f:2f$  frequency chain the latter phase coherently links every laser in the chain to the 10 MHz rf reference that controls the pulse repetition rate and the local oscillators.

To compare the two frequency chains we use the 848 nm laser diode of Fig. 2 and a second 848 nm laser diode locked to the frequency comb of the  $f:2f$  chain. The frequencies of these two laser diodes measured relative to the quartz are 353 504 624 750 000 Hz and 353 504 494 400 000 Hz for the  $f:2f$  and the  $3.5f:4f$  chains, respectively. So we expect a beat note of 130.35 MHz that we measure with a radio frequency counter (Hewlett Packard, model 53132A) referenced to the same quartz oscillator. To avoid cycle-slipping events

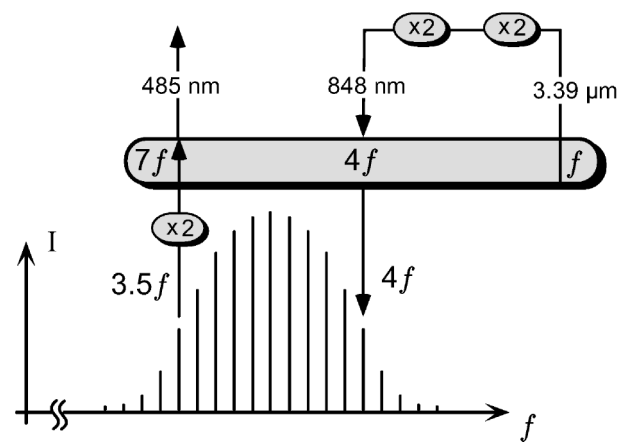


FIG. 2. The first realization of the novel frequency chain that has been used in Refs. [5,22] uses an optical frequency interval divider (oval symbol) [24] that fixes the relation between the frequencies  $f$ ,  $4f$ , and  $7f$ . The 3.39  $\mu$ m laser at  $f$  is locked through the divider after the frequency comb locked  $3.5f$  on  $4f$ .

entering our data we continuously monitor all in-lock beat signals with additional counters that are started shortly before and stopped shortly after the recording of any data point. If one of these counters displays a frequency different from the local oscillator frequency we exclude this point from evaluation. The cycle slip threshold was set to 1 Hz for a counter gate time of 1 s and was reduced as the inverse of the gate time for longer gate times. Because of the small servo bandwidth of the HeNe laser lock, it was operated with a 1024-cycle phase detector [20]. This servo showed by far the largest phase excursions so that the cycle slip threshold was set to 40 times the value of the other phase locked loops.

After averaging all data we obtained a mean deviation from the expected beat frequency of  $71 \pm 179$  mHz at 354 THz. This corresponds to a relative uncertainty of  $5.1 \times 10^{-16}$ . No systematic effect is visible at this accuracy and the distributions of data points look almost ideally Gaussian. The results are summarized in Table I. Figure 3 shows the measured Allan standard deviation for counter gate times of 1, 3, 10, 30, and 100 s. As both 354 THz signals are phase locked to each other (via the quartz oscillator) and the rms phase fluctuation is expected to be constant in time, the Allan standard deviation should fall off like the inverse counter gate time. The large margin phase detector together with the slow servo controlling the phase of the HeNe laser relative to the diode lasers causes frequency fluctuations of 14 Hz at 1 s gate time as measured from the in-lock beat signal. Instabilities could be caused not only by the large margin phase locked loops and slow servos but also by mechanical vibrations or thermal expansion. Note that the large frequency chain of Fig. 2 is resting on two separate optical tables whose relative position is not controlled. Another source of instability could be the specified  $1.5 \times 10^{-13}$  Allan standard deviation (within 1 s) of the quartz oscillator together with time delays present in both systems. To check whether or not the synthesizers

TABLE I. Summary of results from the frequency chain comparison with statistical uncertainties derived from the data. Two additional points have been removed from the 1 s data set that have been more than 50 kHz off but have not been detected as cycle slips. The weighted mean of column 3 yields  $71 \pm 179$  mHz ( $5.1 \times 10^{-16}$ ).

Gate time	Allan standard deviation	Mean deviation from 130.35 MHz	Relative uncertainty	Approved readings
1 s	$3.3 \times 10^{-13}$	$-1.2 \pm 1.8$ Hz	$5.1 \times 10^{-15}$	4310
3 s	$7.0 \times 10^{-14}$	$-0.54 \pm 1.8$ Hz	$5.1 \times 10^{-15}$	181
10 s	$2.6 \times 10^{-14}$	$207 \pm 376$ mHz	$1.1 \times 10^{-15}$	574
30 s	$1.1 \times 10^{-14}$	$551 \pm 441$ mHz	$1.6 \times 10^{-15}$	65
100 s	$3.9 \times 10^{-15}$	$-82 \pm 233$ mHz	$6.6 \times 10^{-16}$	39

introduce additional noise we operated both chains with the same synthesizer to stabilize the repetition rates without any significant difference.

To summarize, we have realized a compact  $f:2f$  interval frequency chain, evaluated its performance, and operated it fully phase locked over periods of hours. It occupies only 1 square meter on our optical table with considerable potential for further miniaturization. At the same time it supplies us with a reference frequency grid across much of the visible and infrared spectrum with modes that are separated by 625 MHz and can easily be distinguished with a commercial wave meter. This makes it an ideal laboratory tool for precision spectroscopy that is ready to serve as a clockwork in future optical clocks. In the reverse

direction we expect this clockwork to transfer not only the accuracy but also the superior stability of optical oscillators to the rf domain. Other important applications arise in the time domain where the carrier offset slippage frequency is an important parameter and needs to be controlled for the next generation of ultrafast experiments.

We thank F. Krausz and A. Poppe (Vienna, Austria), as well as S. Diddams and J. Hall (Boulder, Colorado, USA), for fruitful discussions.

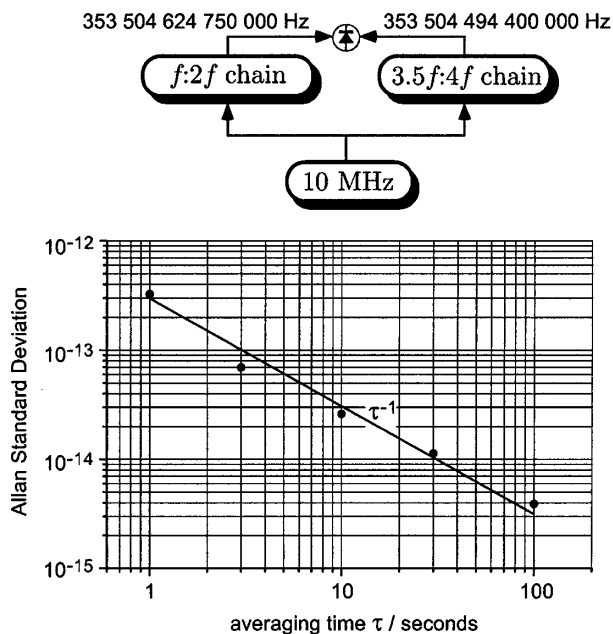


FIG. 3. Top: The setup is shown schematically with the  $f:2f$  and the  $3.5f:4f$  chains as detailed in Figs. 1 and 2, respectively. The graph below shows the measured relative Allan standard deviation derived from the comparison of the two frequency chains. The values are also stated in Table I.

- [1] Th. Udem *et al.*, Phys. Rev. Lett. **79**, 2646 (1997).
- [2] H. Schnatz *et al.*, Phys. Rev. Lett. **76**, 18 (1996).
- [3] C. Schwob *et al.*, Phys. Rev. Lett. **82**, 4960 (1999).
- [4] J. E. Bernard *et al.*, Phys. Rev. Lett. **82**, 3228 (1999).
- [5] J. Reichert *et al.*, Phys. Rev. Lett. **84**, 3232 (2000).
- [6] S. A. Diddams *et al.*, Phys. Rev. Lett. **84**, 5102 (2000).
- [7] D. Jones *et al.*, Science **288**, 635 (2000).
- [8] J. N. Eckstein, A. I. Ferguson, and T. W. Hänsch, Phys. Rev. Lett. **40**, 847 (1978).
- [9] Th. Udem *et al.*, Phys. Rev. Lett. **82**, 3568 (1999).
- [10] S. A. Diddams *et al.*, Opt. Lett. **25**, 186 (2000).
- [11] Th. Udem *et al.*, Opt. Lett. **24**, 881 (1999).
- [12] R. Holzwarth *et al.* (to be published).
- [13] See contributions of T. W. Hänsch *et al.*, in *The Hydrogen Atom* (Springer, Berlin, 1989), and references therein; D. J. Wineland, *ibid.*
- [14] J. C. Knight *et al.*, Opt. Lett. **21**, 1547 (1996).
- [15] M. J. Gander *et al.*, Electron. Lett. **35**, 63 (1999).
- [16] J. K. Ranka, R. S. Windeler, and A. J. Stentz, Opt. Lett. **25**, 25 (2000).
- [17] W. J. Wadsworth *et al.*, Electron. Lett. **36**, 53 (2000).
- [18] A. Apolonski *et al.*, Phys. Rev. Lett. **85**, 740 (2000).
- [19] J. Reichert *et al.*, Opt. Commun. **172**, 59 (1999).
- [20] M. Prevedelli, T. Freearge, and T. W. Hänsch, Appl. Phys. B **60**, S241 (1995).
- [21] L. Xu *et al.*, Opt. Lett. **21**, 2008 (1996).
- [22] M. Niering *et al.*, Phys. Rev. Lett. **84**, 5456 (2000).
- [23] C. Zimmermann *et al.*, Appl. Phys. Lett. **66**, 2318 (1995).
- [24] D. McIntyre and T. W. Hänsch, in *Digest of the Annual Meeting of the Optical Society of America* (Optical Society of America, Washington, DC, 1988); H. R. Telle, D. Meschede, and T. W. Hänsch, Opt. Lett. **15**, 532 (1990).